

UHF Deployable Helical Antennas for CubeSats

Joseph Costantine, Youssef Tawk, Ignacio Maqueda, Maria Sakovsky, Gina Olson,
Sergio Pellegrino, and Christos G. Christodoulou, *Fellow, IEEE*

Abstract—The design process and the deployment mechanism of a quadrifilar helix antenna (QHA) and a conical log spiral antenna (CLSA) are presented. The two antennas are proposed to operate in the UHF frequency band. They are composed of conductors that are embedded and supported by innovative structural techniques. This allows efficient folding, packaging, and deployment once in space. The conductors in the QHA are composed of beryllium copper and are supported by helical arms of S_2 glass fiber reinforced epoxy. The CLSA, on the other hand, has conductors that are made out of a mesh of phosphor bronze and incorporated inside thin insulators composed of continuous fiber composites. The new aspects of these designs lie in their structures and deployment mechanisms. The deployment mechanisms for both antennas include helical pantograph and origami patterns such as Z-folding configurations. Both antennas are fabricated and tested for both deployment and radiation performance. A comparison is executed between both designs, and their potential deployment possibilities from CubeSats are also investigated.

Index Terms—Balun, conical log spiral antenna (CLSA), CubeSat, deployable antennas, helical antennas, helical pantograph, origami, quadrifilar helix antenna (QHA), space communications, Z-folding.

I. INTRODUCTION

THE design of novel space antenna concepts that cover different frequency ranges constitutes a major challenge. There is a rise in the development of nanosatellites such as CubeSats, due to their ease of fabrication and low cost. The push for CubeSat designs has forced antenna designers and aerospace engineers to seek solutions for deployable antennas that have to be stowed inside the CubeSat's limited space and deploy from its platform once in space. The antennas proposed

Manuscript received July 17, 2015; revised March 14, 2016; accepted May 28, 2016. Date of publication June 21, 2016; date of current version September 1, 2016. This work was supported by the Air Force Office of Scientific Research under Grant FA9550-13-1-0061.

J. Costantine is with the Electrical and Computer Engineering Department, American University of Beirut, Beirut 1107-2020, Lebanon, and also with COSMIAC, Albuquerque, NM 87131 USA (e-mail: jcostantine@ieee.org).

Y. Tawk is with the Electrical and Computer Engineering Department, Notre Dame University, Louaize, Lebanon, and also with COSMIAC, Albuquerque, NM 87131 USA (e-mail: yatawk@ieee.org).

I. Maqueda is with the Graduate Aerospace Laboratory, California Institute of Technology, Pasadena, CA 91125 USA, and also with Comet Ingeniería, Valencia, Spain (e-mail: imaqueda@caltech.edu).

M. Sakovsky and S. Pellegrino are with the Graduate Aerospace Laboratory, California Institute of Technology, Pasadena, CA 91125 USA (e-mail: msakovsk@caltech.edu; sergiop@caltech.edu).

G. Olson is with Meggitt Polymers and Composites, McMinnville, OR 97128 USA (e-mail: olsongm@gmail.com).

C. G. Christodoulou is with the Electrical and Computer Engineering Department, University of New Mexico, Albuquerque, NM 87131 USA (e-mail: christos@unm.edu).

Color versions of one or more of the figures in this paper are available online at <http://ieeexplore.ieee.org>.

Digital Object Identifier 10.1109/TAP.2016.2583058

have to be folded in order to fit inside a CubeSat. 1U CubeSats are of the dimensions $10\text{ cm} \times 10\text{ cm} \times 10\text{ cm}$. In this paper, the antennas presented are designed to deploy from a 6U CubeSat and need to be folded to fit inside a 2U CubeSat.

The challenge of deploying antennas from a CubeSat is amplified by the requirements to design antennas that are operational at UHFs. Lower frequencies impose larger antenna sizes. This fact forces the use of extreme packaging ratios and advanced deployment mechanisms.

Many types of deployable antennas have been used on orbit. Reflector types constitute the widest category [1], [2]. These are commonly based on truss types to constitute a synthetic aperture radar that can be mounted on any spacecraft as discussed in [3]. Folded structures that resort to hoops or ribs have been proposed for space communications in [4]. Accordion or spring-shaped tunable antenna structures can also be used on satellite platforms [5]–[7]. Tape springs and neutrally stable material have constituted a major contributor to deployable antenna structure designs as discussed in [8].

Despite the advancement in antenna structure design, the most common antennas deployed on CubeSats remain mainly dipoles that are arrayed in various configurations [9]. Helical antennas are also a popular choice of CubeSat antennas due to their natural circular polarization and wide bandwidth [10]. Patch antennas printed on CubeSat sides are good potential candidates for use on small satellites as discussed in [11].

Deployable antennas for CubeSats can also be designed using log periodic structures such as a log periodic crossed dipole antenna array [12]. The log periodic crossed dipole antenna array can be built using a bistable composite material. This type of antenna exhibits a directive beam and an acceptable bandwidth [12]. Another logarithmically scaled antenna can be the conical log spiral antenna (CLSA) that is typically fed at its apex. This antenna satisfies all the imposed constraints of CubeSat communication operation such as circular polarization, large bandwidth, and efficient gain. Other configurations of the CLSA can also be utilized to satisfy various constraints such as a narrower base or a bigger height. For example, a bottom fed CLSA deployed on top of a ground plane is a possible candidate [13].

This paper discusses antennas with an objective to establish an earth-space satellite link that is operational for transmit and receive between 300 and 600 MHz within the UHF band. The antennas presented are proposed to be circularly polarized since circular polarization is required due to Faraday rotation effects in the ionosphere. This paper considers two classical antenna designs for the CubeSat series of satellites, one narrow-band antenna and one wideband antenna. The narrow-band antenna is a quadrifilar helix antenna (QHA) with

a bandwidth of 22 MHz; here, we choose the operating center frequency to be at 365 MHz. The wideband antenna, a CLSA, is capable of operating over the entire UHF satcom band. These antennas are generally required to have a minimum gain of 5 dB, which can be considered acceptable for a typical UHF CubeSat operation as described in [14]. The antennas are also required to have a maximum axial ratio of 3 dB to satisfy circular polarization requirements. The deployment mechanisms of both antennas allow for a compact storage capability, which is a critical requirement for CubeSat antennas. The QHA is designed using beryllium and is proposed to deploy on top of a deployable ground plane. The CLSA is proposed to be Z-folded once in storage. The antenna then deploys away from the satellite exhibiting typical CLSA behavior.

In this paper, Section II discusses the physical structure of the QHA, its fabrication, as well as its folding and deployment techniques. Section III presents the structure, design, packaging, and deployment of the CLSA. The feeding mechanisms for both antenna structures are shown in Section IV, while Section V details their measurement results and performance analysis. Section VI compares both antenna structures. A discussion about the reliability, accuracy, and feasibility of both proposed antenna designs is executed in Section VII. Section VIII concludes this paper.

II. QUADRIFILAR HELIX ANTENNA STRUCTURE, DESIGN, FABRICATION, AND DEPLOYMENT

Four twisted helical arms constitute the structure of a QHA. The arms are composed of wires that helically wrap around each other forming four orthogonal conductive turns. The arms' conductors are fed in a progressive quadrature phase, and are arranged to define two separate helically twisted loops. A QHA can be described as a collection of four helices that share the same longitudinal axis, and each of the helices is rotated 90° with respect to any of the other three helices. The antenna's topology makes its radiation pattern omnidirectional with a circular polarization. The quadrifilar helix can be fed at the top or at the bottom of the antenna, while the opposite end of the wire is either shorted or open [15], [16].

In this paper, we present a new open-ended QHA. The antenna has four arms of the same lengths and is designed to operate in the UHF band at 365 MHz. The antenna is conceptualized to be deployed using four helical conductive beryllium arms and four additional helical arms that are made of unidirectional S₂ glass composites as shown in Fig. 1(a). The antenna has a helix diameter of 11.52 cm. The helix diameter is the distance between the end tips of two diametrically opposite conductors. The helix height that is the distance from the ground plane to the end of each conductor is 50 cm. The antenna has 1.125 turns and a helix spacing of 37.067 cm.

The dimensions of the supporting nonconducting arms are chosen in a way to achieve sufficient torsional and axial stiffness using geometric and material parameters [17]. During launch, the antenna is compactly stowed and deploys once on orbit. The deployment mechanism summarized in Fig. 2 is based on the helical pantograph concept, which is extended from the linear pantograph concept discussed in [18] and [19]. The conductors are folded elastically into a four-leaf clover

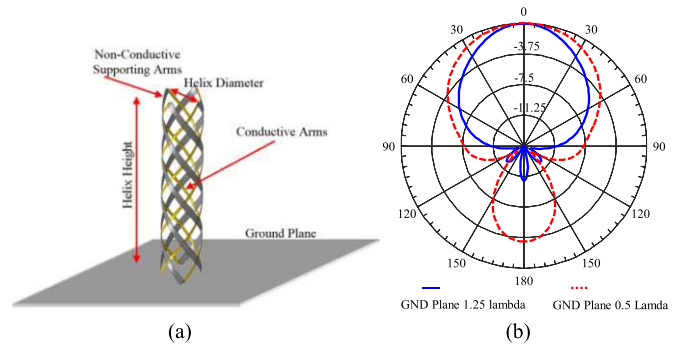


Fig. 1. (a) Antenna structure with conductive arms shown in thin lines and nonconductive supporting arms shown in thick lines. (b) Comparison between the radiation patterns for a ground plane of size 0.5λ and 1.25λ.

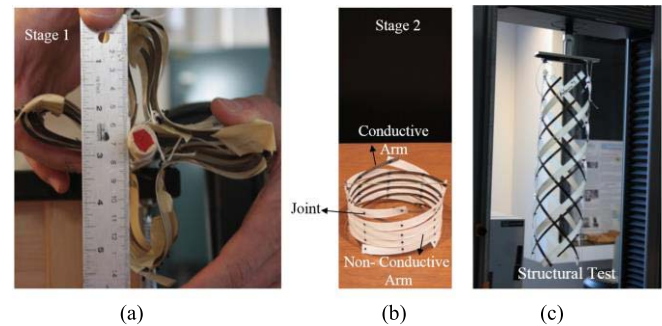


Fig. 2. Fabricated prototype in various stages of deployment.(a) Antenna fully folded at stage 1. (b) Stage 2 of antenna deployment. (c) Antenna fully deployed undergoing a structural test at stage 3

shape as shown in Fig. 2(a). Every beryllium conductor is attached to two supporting helical rods of S₂ glass composite. Multiple nonconductive joints can be used to connect the conductive arms with the nonconductive supporting helices as shown in Fig. 2(b). The dimensions of the joints and the diameters of the holes drilled to attach them are in the order of λ/200 at 365 MHz. The opposite sense helices that are connected by joints are also aligned with the radial direction, at every crossover point as shown in Fig. 2(c). Unlike the linear pantograph, this structure undergoes elastic deformation to achieve relative rotation of the joints. Hence, the structure has the potential to deploy by releasing its stored strain energy, rather than relying on deployment systems that provide external energy, such as cables or motors. It is also capable of significant length changes during the stowing and deployment phases. These features extend beyond many other techniques that are applied on antennas with similar topologies [19].

The conductive and support helices are strain free after deployment. The eight-helix helical pantograph is tested for deployment functionality and compaction force. The helices are attached with nonconductive screws, and thin plastic washers are used to separate the helices at all connection points in order to reduce friction. In the fabricated prototype shown in Fig. 2(c), the beryllium conductors are colored in gold, while the support helices are colored in white.

In order to avoid any antenna radiation to be directed toward the satellite, a ground plane is required to be deployed underneath the antenna. The size of the ground plane is

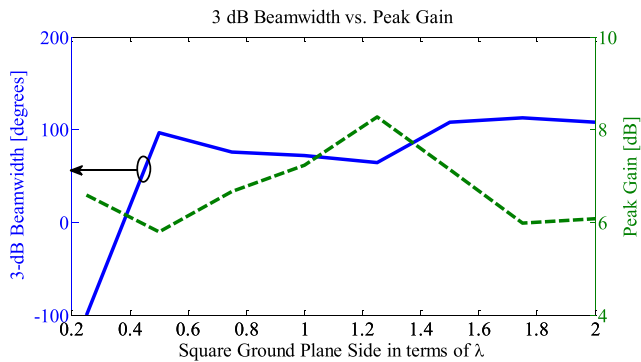


Fig. 3. 3-dB beamwidth versus peak gain in function of ground plane side dimension [15].

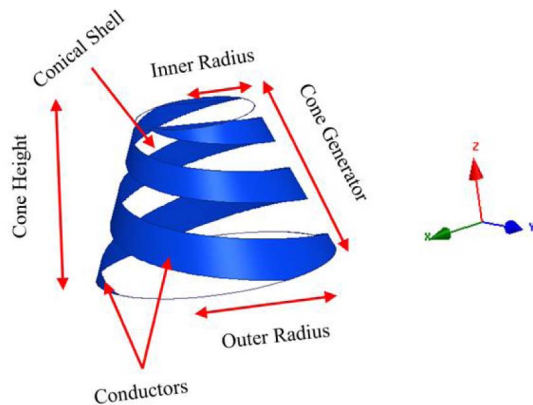


Fig. 4. CLSA design parameters.

a key aspect in the design process of such structures. It is found through an iterative optimization analysis using Ansys' HFSS [20] that the dimensions of the ground plane affect the antenna's back lobe radiation, beamwidth, and peak gain. The effect of the ground plane size on the gain and 3-dB beamwidth is shown in Fig. 3. A peak gain of 8 dB is reached when the side of the square ground plane is 1.25λ . However, the 3-dB beamwidth reaches its peak of 100° at around 0.5λ [15]. As for the back lobe radiation, it is inversely proportional to the size of the ground plane. Fig. 1(b) shows a comparison between the radiation patterns of the QHA for a ground plane of sizes 0.5λ and 1.25λ .

III. CONICAL LOG SPIRAL ANTENNA DESIGN, STRUCTURE, AND DEPLOYMENT

Another candidate proposed for deployment from a CubeSat is the CLSA. A CLSA is defined as a frequency-independent antenna [21]. The CLSA is composed of conductors that wrap around a conically shaped structure in a logarithmically progressive manner.

The operating frequency of a CLSA is dependent on the ratio between the outer and the inner radii of the cone defining the structure [21]. The outer radius is the radius of the base of the cone (large radius), while the inner radius is the radius of the circle at the apex of the cone (smaller radius). The structure of the CLSA is shown in Fig. 4. The increase in the

ratio between these two radii improves the performance of the antenna at lower frequencies. As any logarithmic antenna, the topology of the radiating conductor heavily affects the antenna radiation characteristics. In this case, the winding of the conductor determines its directivity [21]. The radiation characteristics of the antenna are determined by a study of its propagation constant. This has led to the identification of the antenna's active region, also known as the antenna's effective radiating aperture. Any CLSA design depends on the position and size of this active region as a function of the various antenna parameters [21].

One of the most important parameters in the design of the CLSA is the cone generator. The cone generator is optimized to be 19.6 cm using Ansys' HFSS [20], to satisfy both electromagnetic performance and structural packaging constraints. The antenna is logarithmically scaled, which forces its conductors' widths, and the spacing between the different conductors' turns to be logarithmically distributed.

The CLSA is typically fed at its apex. This feeding topology ensures that the radiation is directed towards the apex of the cone that governs the antenna structure. No significant back radiation must be noted. The ability of the CLSA to radiate, in its majority, toward its apex with an insignificant back lobe radiation allows it to be a suitable candidate for CubeSat deployment. The antenna design proposed herein has an inner radius of 7 cm, an outer radius of 14.1 cm, 1.25 turns of the conductor, and a cone height of 18.5 cm.

The major novel aspects of this antenna design are its structure, deployment mechanism, and material composition. The structure of the proposed CLSA has to be stowed compactly while in storage and then deploy once in space. In order for the antenna to possess such properties, it has to exhibit high packing ratios during storage and great deployment reliability once in space. The material used to fabricate the antenna as well as its structural composition has to allow this desired structural behavior. Thus, the antenna is built using a support material that is composed of a dual-matrix shell [22], [23]. The shell is composed of fiberglass, epoxy, and ultraviolet (UV) cured silicone. The epoxy used is the PMT-F4 from Patz Technologies. The silicone used is the UV-curing silicone LOCTITE 5055 [24], and the fiberglass used is the Astroquartz II 525 plain weave fabric from JPS Composites.

The conductor used to form the radiator of the CLSA is a phosphor bronze-woven mesh from TPW, Inc. Thus, the conductor is not a continuous filament but rather a mesh of microwires that are woven together with an average of 325 wires/in and a wire diameter of $28 \mu\text{m}$. The conductor needs to be thin to minimize its effect on the folding capabilities of the dual-matrix shell. However, its thickness needs to be larger than the skin depth (δ) [25] of the conductor at the lowest operating frequency. In this paper, the thickness of the conductor is chosen to be around 2δ , which is equivalent to $6 \mu\text{m}$. The phosphor bronze mesh conductor is sandwiched between two layers of Astroquartz-epoxy composites that are impregnated at the folding locations with an Astroquartz-silicone composite.

The fabricated prototype shown in Fig. 5 is composed of a six-ply plain weave fiberglass. The antenna is required to

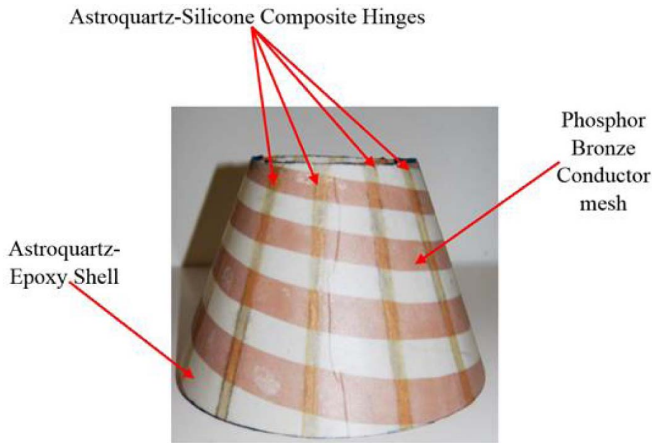
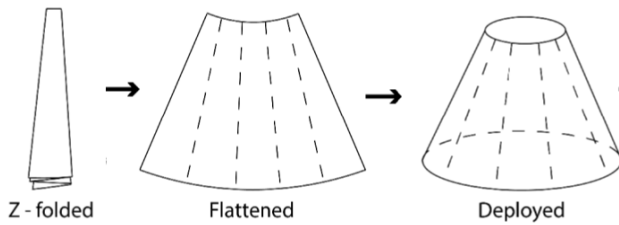


Fig. 5. Fabricated CLSA.



(a)



(b)

Fig. 6. (a) Z-folding progression scheme. (b) Implementation of the folding process on the fabricated prototype.

be folded and stowed during the launch phase. The folding mechanism that is proposed to be applied on this type of antenna is the Z-folding scheme. It is based on the fact that the Astroquartz-silicone composite infused in strategic locations acts as hinges that allow the origami Z-folding mechanism to occur as shown in Fig. 6. The folding lines that are composed of an Astroquartz-silicone composite are 10-mm wide and are embedded in a silicone matrix. The remainder of the shell is embedded in a stiffer epoxy matrix.

Based on the fact that the CLSA radiates toward its apex with no significant back lobe radiation, a ground plane is not needed for deployment in this case. The antenna is also proposed to deploy and reach its final stable configuration as shown in Fig. 7 where the deployed CLSA is integrated with a 6U CubeSat. A dual-matrix composite based on Astroquartz support rod deploys the Z-folded antenna from the satellite cavity and maintains the stability of the antenna once on orbit. The presence of the satellite as well as the rod affects the

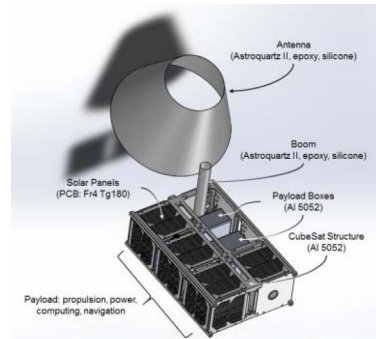


Fig. 7. Diagram of a 6U CubeSat with the deployed CLSA.

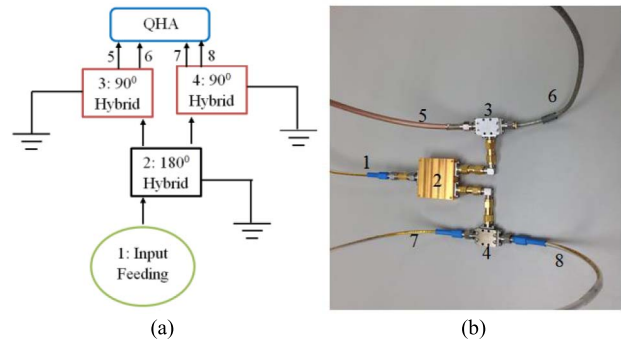


Fig. 8. QHA's feeding network. (a) Diagram. (b) Implementation.

antenna radiation characteristics. The rod dimensions, tilting angle, and the satellite's position with respect to the antenna are optimized in order to reduce their effect on the antenna's back lobe radiation, circular polarization, gain, and operating bandwidth. It is found that a minimum effect is achieved with a rod of radius 1 cm and a total length 20 cm, out of which only 10 cm extends outside the satellite. The overlap between the antenna's nonconductive shell and the rod is optimized to be at a maximum of 2 cm. The rod has to also be titled out of the satellite with an angle of at least 20°. It is important to note that similar to the QHA, the dual-matrix shell composing the antenna can also deploy using only stored energy and does not require any actuation.

IV. FEEDING MECHANISMS

A. Feeding Network for the Quadrifilar Helix Antenna

The feeding network of a QHA has to allow a quadrature phase difference between each pair of the conducting arms. The objective is to achieve a progressive 90° phase shift between the different ports of the antenna. The power fed to the antenna's input port is redistributed as well as phase shifted among the different antenna arms. The feeding network adopted for this design consists of a one-to-two-port 180° hybrid coupler with a power splitter and two 90° hybrid couplers with power splitters, as summarized in Fig. 8(a). Each output port of the 180° hybrid coupler is connected to an input port of the 90° hybrid coupler. The different ports of the 90° hybrid couplers excite the antenna arms with a progressive 90° phase shift [26]. It is important to note that since this antenna deploys vertically on top of a ground plane, the feeding network is proposed to be included inside the

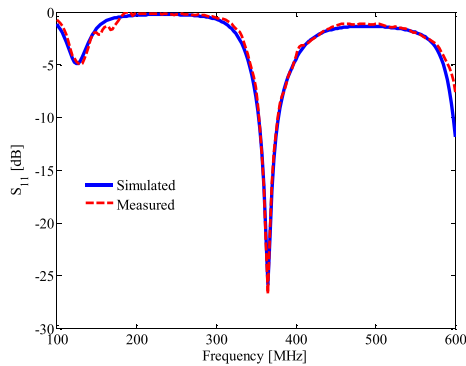


Fig. 9. Measured and simulated reflection coefficient for the QHA.

satellite cavity at all time and does not deploy with the antenna itself. The actual implementation of the feeding network is presented in Fig. 8(b).

B. Feeding Network for the Conical Log Spiral Antenna

The CLSA is a dual-armed antenna with a differential input impedance of 200Ω . The phase shift between each arm of the antenna is 180° . In order to properly excite the active region of this antenna, a balun is required. The balun divides the power equally among the two arms of the antenna, properly providing the antenna with the appropriate impedance, and accurately creating a 180° phase between the two antenna arms. A 50/200 surface mounted device (SMD) balun is used in this setup [27]. The balun is chosen to be operational over the UHF band from 150 to 650 MHz [27]. A 50- Ω SMA connector feeds a planar 50- Ω microstrip line that is soldered to the input of the balun. The two output pins of the balun are connected to two microstrip lines with a characteristic impedance of 100Ω each. The microstrip lines at the output are then connected to two coaxial cables of the same length and with a 100- Ω characteristic impedance each. The coaxial cables are then led from inside the antenna structure into the apex of the cone where they feed simultaneously the two arms of the antenna. Fig. 6 shows the antenna Z-folded and fully deployed while fed with the coaxial cables and the feeding network. The antenna is folded while maintaining the feeding network and cables connected to the top apex of the structure as shown in Fig. 6.

V. MEASUREMENTS, OPERATION, AND RESULTS

A. Performance of the Quadrifilar Helix Antenna

The QHA is measured on top of a square ground plane with a side of 1.25λ (1.02 m). The antenna's measured reflection coefficient presents good agreement with the simulated one, as shown in Fig. 9. The QHA operates between 352 and 378 MHz with a center frequency at 365 MHz and 7.12% bandwidth. The QHA's measurement setup is shown in Fig. 10(a), and the gain pattern of the antenna is highlighted in Fig. 10(b). A peak gain of 8.38 dB is achieved at $f = 365$ MHz. The antenna is also circularly polarized with an axial ratio that is below 3 dB at 365 MHz and throughout the whole radiation beamwidth as shown in Fig. 11(a). Fig. 11(b) shows the axial ratio across the complete operational bandwidth of the QHA proving that the antenna is circularly polarized across the full frequency span.

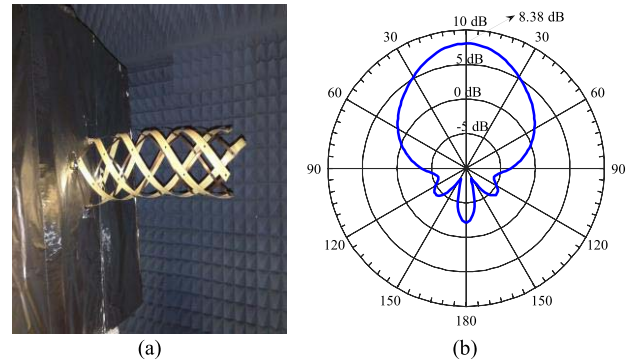


Fig. 10. (a) QHA's measurement setup. (b) Gain pattern at 365 MHz for the XZ and YZ plane cuts.

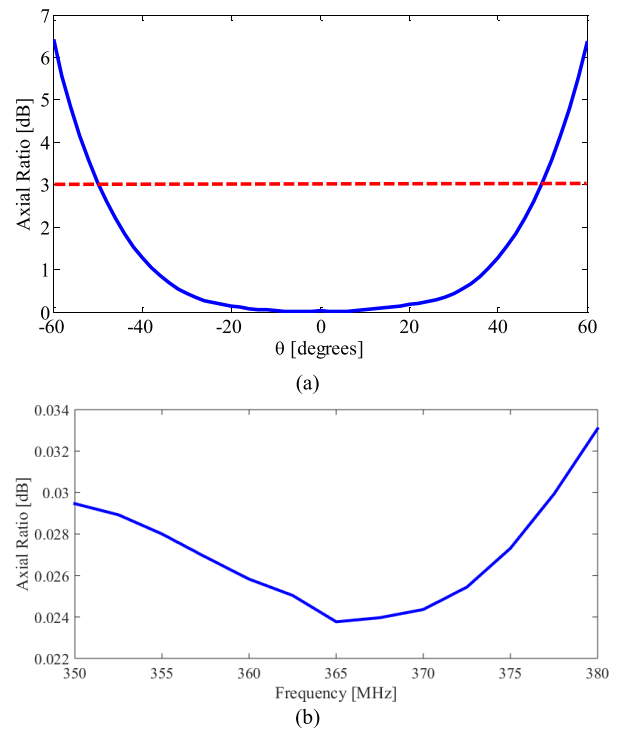


Fig. 11. (a) Axial ratio of the QHA at 365 MHz. (b) Axial ratio for $\theta = \phi = 0^\circ$ throughout the full operational bandwidth.

Structural tests are also executed on the antenna to measure compaction loads and the resulting deformation as shown in Fig. 2(c) [17].

B. Performance of the Conical Log Spiral Antenna

The CLSA is designed to operate in the UHF band between 300 and 650 MHz. The antenna is also designed to have a maximum front lobe radiation out of its apex and a minimum back lobe radiation. The antenna resorts to a commercial balun to appropriately feed its structure. The balun's operational bandwidth is first measured when the designed feeding network is terminated with 100- Ω SMD resistors. The operational bandwidth of the balun is shown in Fig. 12. It is important to indicate that the antenna is designed to operate between 300 and 650 MHz, while the balun allows operation between 150 and 650 MHz [27]. The intersection between the measured antenna performance and the measured balun's bandwidth

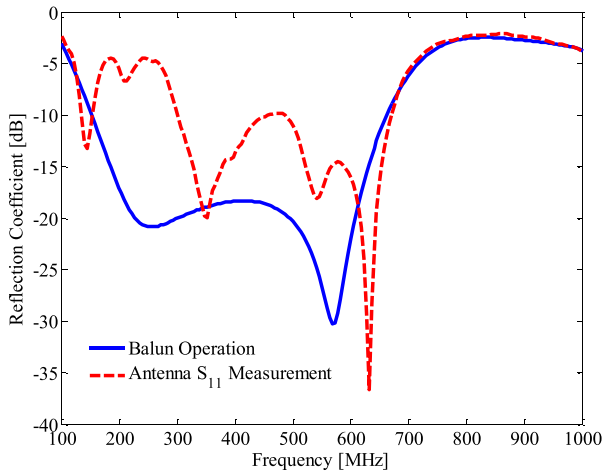


Fig. 12. Comparison between the antenna’s measured reflection coefficient and the balun operational bandwidth.

of operation is shown in Fig. 12. This plot shows that the antenna’s measured performance is within the allowable bandwidth of operation of the balun and thus constitutes a validation of the built antenna prototype with its feeding network. The measurement setup for the antenna deployed from the satellite is shown in Fig. 13(a). The antenna’s gain pattern at 450 MHz is plotted in Fig. 13(b) where maximum radiation is directed toward the apex of the cone with a gain of 5.57 dB. The gain of the CLSA as a function of frequency is shown in Fig. 13(c) for $\theta = \phi = 0^\circ$. Fig. 13(c) shows that the gain of the antenna remains above 5 dB for the full operational bandwidth. The axial ratio of the antenna at 450 MHz for the radiation beamwidth is shown in Fig. 14.

VI. COMPARISON BETWEEN THE QHA AND THE CLSA

A comparison between both types of helical antennas that are presented in this paper needs to take into consideration all the important characteristics that such antennas exhibit and execute a tradeoff analysis between each of them.

- 1) *Bandwidth*: Both antennas are designed to operate in the UHF band of operation; however, the QHA exhibits a single-frequency operation, while the CLSA is more of a wideband antenna due to its logarithmic and frequency-independent structure.
- 2) *Polarization*: Both antennas are circularly polarized due to their helical nature.
- 3) *Radiation Pattern*: The QHA has an omnidirectional pattern; however, the addition of a ground plane that deploys with the antenna allows its directive behavior away from the CubeSat. On the other hand, the CLSA’s radiation pattern is directive away from the satellite without the need for a deployable ground plane underneath its structure.
- 4) *Gain*: The QHA exhibits a higher gain than the CLSA due to its structure composed of four arms. However, it is important to note that the CLSA exhibits an almost constant gain value over the entire bandwidth of operation.
- 5) *Feeding Mechanism*: Both antennas require an appropriately designed feeding network. QHA requires a quadra-

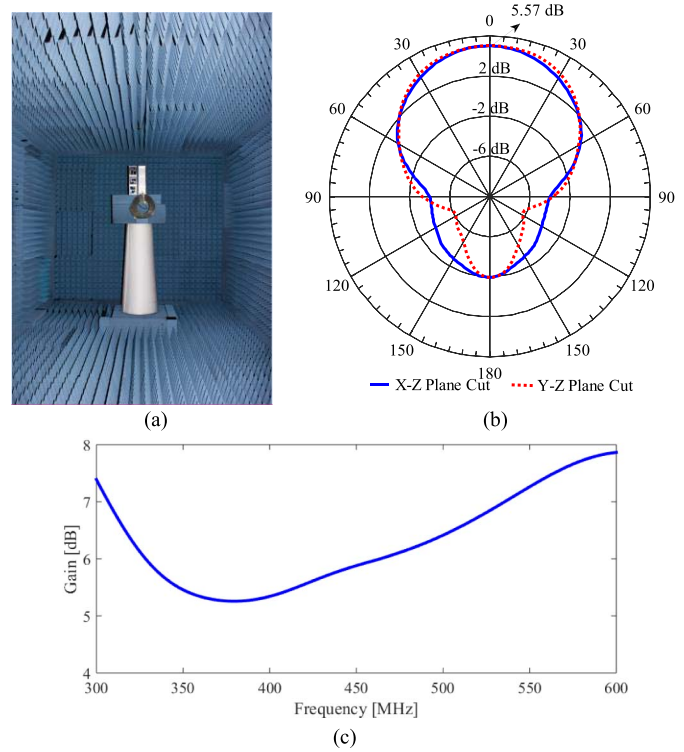


Fig. 13. (a) CLSA’s measurement setup. (b) Antenna gain pattern at 450 MHz in both the XZ and YZ plane cuts. (c) Gain of CLSA versus frequency operation at $\theta = \phi = 0^\circ$.

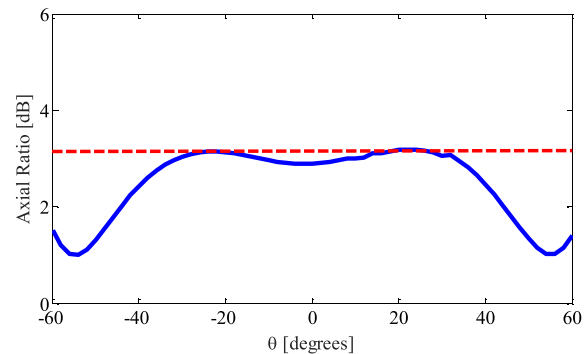


Fig. 14. Axial ratio of the CLSA at 450 MHz for the beamwidth of radiation.

ture progressive phase shift between its constituent elements, while the CLSA requires a balun that provides appropriate impedance matching and power division.

- 6) *Deployment and Folding*: The QHA resorts to helical pantographs for deployment, while the CLSA resorts to flattening and Z-folding patterns. Both antennas exhibit high stiffness and natural frequencies away from the environmental forcing frequencies, which makes them highly stable while deployed.

It is not possible to indicate which antenna is a better candidate for CubeSat deployment. However, the choice of a particular antenna structure highly depends on the requirements imposed by the system itself. A single-frequency system with a higher gain requirement can benefit from a QHA. On the other hand, a wider frequency operation with a lower gain enables the adoption of a CLSA structure. Table I summarizes the comparison between both antenna structures.

TABLE I
COMPARISON BETWEEN QHA AND CLSA'S CHARACTERISTICS

Antenna Characteristic	QHA	CLSA
Bandwidth	Single Frequency	Wide Band
Polarization	Circular	Circular
Radiation Pattern	Needs a ground plane to be directive	Directive without a ground plane
Gain	$\geq 8\text{dB}$	$\geq 5\text{dB}$
Feeding	Progressive Quadrature Phase Shift	Balun Circuit
Deployment and Folding	Pantographs	Z Folding

VII. RELIABILITY, ACCURACY, AND FEASIBILITY

Deployable antennas are required to deploy only once on orbit and then remain deployed without any change until the satellite is out of service. In that sense, the reliability of any deployable antenna can be monitored by its ability to deploy only once and function appropriately. However, in order to ensure the validity of our designs, the reliability of deployment and appropriate functioning are assessed by repeating the stowing and deployment process of each of the antenna prototypes for about 50 times. Every repetition of the deployment and stowing process involves measurement of the antenna's radiation performance as well as its structural strength.

The accuracy of fabrication is also verified by measuring the fabricated dimensions (upper radius, lower radius, and antenna height) of the prototype after 50 consecutive folding and deployment repetitions. It is our conclusion that the accuracy in fabrication for a CLSA that has never been folded is around 98.4%. After 50 consecutive folding and deployment repetitions, the accuracy of the fabricated prototype relative to the design dimensions is comparable at around 97.9%. Similar results are received for the QHA prototype. Such figures are matched by the antenna performance characterization and its agreement with the simulated results.

In terms of feasibility, the fabrication methods used to build both the CLSA and the QHA are similar to the fabrication of any composite material. All fiber material and resin deposits are commercially available, and the process does not require any nontraditional equipment for composite manufacturing ensuring that fabrication is feasible.

VIII. CONCLUSION

The design characteristics of two potential antenna structures to be deployed from CubeSats are discussed in this paper. Helical antenna types appear to be suitable candidates for such a deployment. The design and structure of a QHA and a CLSA are discussed. While both antennas exhibit circular polarization and a high gain, the QHA requires a deployable ground plane for radiation redirection.

The CLSA is a wideband antenna that covers the desired bandwidth, while the QHA restricts its operation to a single frequency. Both antennas resort to advanced folding mechanisms to be able to achieve high packaging ratios during launch. The feeding mechanism of each antenna type is discussed, and a comparison is presented between both antenna candidates.

REFERENCES

- [1] T. Takano *et al.*, "Deployable antenna with 10-m maximum diameter for space use," *IEEE Trans. Antennas Propag.*, vol. 52, no. 1, pp. 2–11, Jan. 2004.
- [2] C. Granet, I. M. Davis, J. S. Kot, and G. S. Pope, "A deployable reflector antenna with a simplified X/Ka simultaneous feed-system," in *Proc. 3rd Eur. Conf. Antennas Propag.*, Mar. 2009, pp. 1176–1178.
- [3] A. S. Chebotarev, V. A. Panteleev, N. M. Feyzulla, E. M. Mitrofanov, and A. N. Plastikov, "Truss-type deployable reflector antenna systems for synthetic aperture radar mounted on a small spacecraft," in *Proc. 24th Int. Crimean Conf. Microw. Telecommun. Technol. (CriMiCo)*, Sep. 2014, pp. 521–522.
- [4] F. Zheng, M. Chen, W. Li, and P. Yang, "Conceptual design of a new huge deployable antenna structure for space application," in *Proc. IEEE Aerosp. Conf.*, Mar. 2008, pp. 1–7.
- [5] S. Yao, X. Liu, S. V. Georgakopoulos, and M. M. Tentzeris, "A novel tunable origami accordion antenna," in *Proc. IEEE Int. Symp. Antennas Propag.*, Jul. 2014, pp. 370–371.
- [6] S. Yao, S. V. Georgakopoulos, B. Cook, and M. M. Tentzeris, "A novel reconfigurable origami accordion antenna," in *Proc. IEEE MTT-S Int. Microw. Symp.*, Jun. 2014, pp. 1–4.
- [7] S. Yao, X. Liu, S. V. Georgakopoulos, and M. M. Tentzeris, "A novel reconfigurable origami spring antenna," in *Proc. IEEE Int. Symp. Antennas Propag.*, Jul. 2014, pp. 374–375.
- [8] T. W. Murphy and S. Pellegrino, "A novel actuated composite tape-spring for deployable structures," Amer. Inst. Aeronautics Astronautics, Reston, VA, USA, Tech. Rep. TR-1528, Apr. 2004.
- [9] P. Muri, O. Challa, and J. McNair, "Enhancing small satellite communication through effective antenna system design," in *Proc. Military Commun. Conf.*, San Jose, CA, USA, Nov. 2010, pp. 347–352.
- [10] H. King and J. Wong, "Characteristics of 1 to 8 wavelength uniform helical antennas," *IEEE Trans. Antennas Propag.*, vol. 28, no. 2, pp. 291–296, Mar. 1980.
- [11] C. G. Kakoyiannis and P. Constantinou, "A compact microstrip antenna with tapered peripheral slits for CubeSat RF Payloads at 436MHz: Miniaturization techniques, design & numerical results," in *Proc. IEEE Int. Workshop Satellite Space Commun. (IWSSC)*, Toulouse, France, Oct. 2008, pp. 255–259.
- [12] J. Costantine, Y. Tawk, C. G. Christodoulou, J. Banik, and S. Lane, "CubeSat deployable antenna using bistable composite tape-springs," *IEEE Antennas Wireless Propag. Lett.*, vol. 11, pp. 285–288, 2012.
- [13] A. J. Ernest, Y. Tawk, J. Costantine, and C. G. Christodoulou, "A bottom fed deployable conical log spiral antenna design for CubeSat," *IEEE Trans. Antennas Propag.*, vol. 63, no. 1, pp. 41–47, Jan. 2015.
- [14] D. Ichikawa, "CubeSat-to-ground communication and mobile modular groundstation development," Dept. Elect. Eng., Univ. Hawaii, Honolulu, HI, USA, Tech. Rep. 16_SUM06-FA06, 2006.
- [15] J. Costantine, Y. Tawk, and C. G. Christodoulou, "A new quadrifilar helix antenna for space communications," in *Proc. IEEE Int. Symp. Antennas Propag.*, Orlando, FL, USA, Jul. 2013, pp. 2067–2068.
- [16] A. Adams, R. Greenough, R. Wallenberg, A. Mendelovicz, and C. Lumjiak, "The quadrifilar helix antenna," *IEEE Trans. Antennas Propag.*, vol. 22, no. 2, pp. 173–178, Mar. 1974.
- [17] G. M. Olson, S. Pellegrino, J. Banik, and J. Costantine, "Deployable helical antennas for CubeSats," in *Proc. 54th AIAA/ASME/ASCE/AHS/ASC Struct., Struct. Dyn. Mater. Conf.*, 2013, pp. 1671–1684.
- [18] Z. You and S. Pellegrino, "Cable-stiffened pantographic deployable structures. I—Triangular mast," *AIAA J.*, vol. 34, no. 4, pp. 813–820, 1996.
- [19] G. Olson, S. Pellegrino, J. Costantine, and J. Banik, "Structural architectures for a deployable wideband UHF antenna," in *Proc. 53rd AIAA/ASME/ASCE/AHS/ASC Struct., Struct. Dyn. Mater. Conf.*, Honolulu, HI, USA, Apr. 2012, pp. 23–26.
- [20] Ansys Inc., accessed on Mar. 14, 2016. [Online]. Available: <http://www.ansys.com/Products/Simulation+Technology/Electronics/Signal+Integrity/ANSYS+HFSS>
- [21] J. Dyson, "The characteristics and design of the conical log-spiral antenna," *IEEE Trans. Antennas Propag.*, vol. 13, no. 4, pp. 488–499, Jul. 1965.
- [22] K. Saito, S. Pellegrino, and T. Nojima, "Manufacture of arbitrary cross-section composite honeycomb cores based on origami techniques," *J. Mech. Design*, vol. 136, no. 5, pp. 051011–051020, 2014.

- [23] A. Todoroki, K. Kumagai, and R. Matsuzaki, "Self-deployable space structure using partially flexible CFRP with SMA wires," *J. Intell. Mater. Syst. Struct.*, vol. 20, no. 12, pp. 1415–1424, 2009.
- [24] *Loctite.Loctite5055*, accessed on Mar. 14, 2013. [Online]. Available: [https://tds.us.henkel.com/NA/UT/HNAUTTDS.nsf/web/88C664FFAF9001438525775E006CE0B0/\\$File/5055-EN.pdf](https://tds.us.henkel.com/NA/UT/HNAUTTDS.nsf/web/88C664FFAF9001438525775E006CE0B0/$File/5055-EN.pdf)
- [25] C. A. Balanis, *Advanced Engineering Electromagnetics*, 2nd ed. New York, NY, USA: Wiley, 2012.
- [26] R. A. Marino, "Quadrifilar helix feed network," U.S. Patent 6480173, Nov. 12, 2002.
- [27] *Anaren*, accessed on Mar. 14, 2016. [Online]. Available: https://www.anaren.com/sites/default/files/B0205F50200AHF_DataSheet_RevA.pdf



Joseph Costantine received the bachelor's degree in electrical, electronics, and computer and communications engineering from the Second Branch, Faculty of Engineering, Lebanese University, Beirut, Lebanon, in 2004, the master's degree in computer and communications engineering from the American University of Beirut, Beirut, in 2006, and the Ph.D. degree from The University New of Mexico, Albuquerque, NM, USA, in 2009.

He has authored many research papers, three patents, two books and one book chapter. His current research interests include reconfigurable antennas for wireless communication systems, cognitive radio, antennas for biomedical applications, and deployable antennas for small satellites.

Prof. Costantine was a recipient of many awards, including the Summer Faculty Fellowship from the Space Vehicles Directorate in Albuquerque from 2011 to 2013.



Yousef Tawk received the B.E. degree (Hons.) from Notre Dame University–Louaize, Zouk Mosbeh, Lebanon, in 2006, the M.E. degree from the American University of Beirut, Beirut, Lebanon, in 2007, and the Ph.D. degree from The University of New Mexico (UNM), Albuquerque, NM, USA, in 2011.

He completed his post-doctoral research with UNM in 2012. He served as the Valedictorian of his graduating class with Notre Dame University–Louaize. He holds three patents and has co-authored two books and one book chapter. His current research interests include software defined radio tools for communication systems, cognitive radio RF front-end, RF electronic design, millimeter-wave systems, deployable antennas, and RF photonics.

Dr. Tawk has received many awards and honors, such as the 2014 UNM STC Innovation Award, throughout his education and career. He has several publications many of which received finalist positions and honorable mentions in several paper contests.



Ignacio Maqueda received the Aerospace Engineering degree from the Universidad Politécnica de Madrid, Madrid, Spain, in 2007, and the M.S. and Ph.D. degrees in aeronautical engineering from the California Institute of Technology, Pasadena, CA, USA, in 2010 and 2014, respectively, as a Fulbright Scholar. Under the supervision of his academic advisor, Prof. S. Pellegrino, his Ph.D. thesis focused on the study of high-strain composites and the development of dual-matrix composites for deployable space structures.

Dr. Maqueda serves as a member of the Executive Board of the Spanish Fulbright Alumni Association.



Maria Sakovsky received the B.A.Sc. degree in aerospace engineering from the University of Toronto, Toronto, ON, Canada, in 2013, and the master's degree in space engineering from the California Institute of Technology, Pasadena, CA, USA, in 2014, where she is currently pursuing the Ph.D. degree with the Space Structures Laboratory.

Her current work is on the application of dual-matrix composites to high-performance antenna structures for CubeSats, focusing on experimental and finite element characterization of these materials. Her current research interests include deployable composite structures.



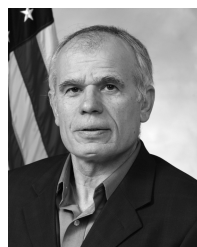
Gina Olson received the B.S. degree in mechanical engineering from the Rose-Hulman Institute of Technology, Terre Haute, IN, USA, and the M.S. degree in aeronautical engineering from the California Institute of Technology, Pasadena, CA, USA.

Her current research interests include deployable structures and high strain composites. She is currently a Technical Lead Engineer with Meggitt Polymers and Composites, McMinnville, OR, USA.



Sergio Pellegrino received the Laurea degree in civil engineering from the University of Naples, Naples, Italy, in 1982, and the Ph.D. degree in structural mechanics from the University of Cambridge, Cambridge, U.K., in 1986.

He is currently the Joyce and Kent Kresa Professor of Aeronautics and a Professor of Civil Engineering with the California Institute of Technology, Pasadena, CA, USA, and a Jet Propulsion Laboratory Senior Research Scientist. His current research interests include the mechanics of lightweight structures, with a focus on packaging, deployment, shape control, and stability.



Christos G. Christodoulou (F'02) received the Ph.D. degree in electrical engineering from North Carolina State University, Raleigh, NC, USA, in 1985.

He served as a Faculty Member with the University of Central Florida, Orlando, FL, USA, from 1985 to 1998. In 1999, he joined the faculty with the Electrical and Computer Engineering Department, The University of New Mexico (UNM), Albuquerque, NM, USA, where he served as the Chair of the Electrical and Computer Engineering Department from 1999 to 2005. He is currently a Distinguished Professor with UNM. He is the Associate Dean of Research with the School of Engineering, UNM, and one of the founders of COSMIAC at UNM. He has authored about 500 papers in journals and conferences, has 17 book chapters, and has co-authored eight books. His current research interests include modeling of electromagnetic systems, cognitive radio, and machine learning in electromagnetics, high power microwave antennas, and reconfigurable antennas for cognitive radio.

Dr. Christodoulou is a member of the Commission B of URSI. He was a recipient of the 2010 IEEE John Krauss Antenna Award for his work on reconfigurable fractal antennas using MEMS switches, the Lawton-Ellis Award, and the Gardner Zemke Professorship at UNM.